Analytic Density-Functional Theory Calculations of Pure Vibrational Hyperpolarizabilities: The First Dipole Hyperpolarizability of Retinal and Related Molecules

Bin Gao,[†] Magnus Ringholm,[†] Radovan Bast,[‡,§] Kenneth Ruud,[*,†] Andreas J. Thorvaldsen,[†] and Michał Jaszuński[¶]

Centre for Theoretical and Computational Chemistry, Department of Chemistry, University of Tromsø—The Arctic University of Norway, N–9037 Tromsø, Norway, Laboratoire de Chimie et Physique Quantiques, CNRS/Université de Toulouse 3 (Paul Sabatier), 118 route de Narbonne, F–31062 Toulouse, France, and Institute of Organic Chemistry, Polish Academy of Sciences, Kasprzaka 44, 01-224 Warsaw, Poland

E-mail: kenneth.ruud@uit.no

---

[*] To whom correspondence should be addressed

[†] Centre for Theoretical and Computational Chemistry, Department of Chemistry, University of Tromsø—The Arctic University of Norway, N–9037 Tromsø, Norway

[‡] Laboratoire de Chimie et Physique Quantiques, CNRS/Université de Toulouse 3 (Paul Sabatier), 118 route de Narbonne, F–31062 Toulouse, France

[¶] Institute of Organic Chemistry, Polish Academy of Sciences, Kasprzaka 44, 01-224 Warsaw, Poland

[§] Present address: Department of Theoretical Chemistry and Biology, Royal Institute of Technology, Roslagstullsbacken 15, S–106 91 Stockholm, Sweden

Abstract

We present a general approach for the analytic calculation of pure vibrational contributions to the molecular (hyper)polarizabilities at the density-functional level of theory. The analytic approach allows us to study large molecules, and we apply the new code to the study of the first dipole hyperpolarizabilities of retinal and related molecules. We investigate the importance of electron correlation as described by the B3LYP exchange–correlation functional on the pure vibrational and electronic hyperpolarizabilities, and compare the computed hyperpolarizabilities with available experimental data. The effects of electron correlation on the pure vibrational corrections vary signficantly even between these structurally very similar molecules, making it difficult to estimate these effects without explicit calculations at the density-functional theory level. As expected, the frequency-dependent first hyperpolarizability, which determines the experimentally observed second-harmonic generation, is dominated by the electronic term, whereas for the static hyperpolarizability the vibrational contribution is equally important. As a consequence, frequency extrapolation of the measured optical hyperpolarizabilities can only provide an estimate for the electronic contribution to the static hyperpolarizability, not its total value. The relative values of the hyperpolarizabilities for different molecules, obtained from the calculations, are in reasonable agreement with experimental data.

Keywords: retinol, retinoic acid, vitamin A acetate, retinal Schiff base, protonated retinal Schiff base, second-harmonic generation

Introduction

A number of theoretical studies have demonstrated the importance of so-called pure vibrational contributions to (hyper)polarizabilities.[1] These contributions can in many cases be significant and in the static case even dominate over the electronic contribution to the hyperpolarizabilities.[2,3] However, for optical frequencies these vibrational contributions are damped, and for processes only involving optical frequencies, such as second-harmonic generation, pure vibrational contributions are in most cases found to be negligible. This implies that the extrapolation procedure often used in experiment to extract static hyperpolarizabilities will never be able to recover the static hyperpolarizability, only the electronic contribution to the first hyperpolarizability. Theoretical studies of pure vibrational and electronic hyperpolarizabilities are thus required in order to shed light on the true static limit of nonlinear hyperpolarizabilities.

The pure vibrational contributions arise from excitations within the vibrational manifold of the electronic ground state instead of excitations within the manifold of electronic excited states, as is the case for the electronic contributions to the hyperpolarizabilites.[1]

The perturbation theory approach by Bishop and Kirtman was a major step forward in order to allow pure vibrational contributions to the (hyper)polarizabilities to be studied in polyatomic molecules.[4,5] By considering the geometry dependence of the electric dipole operator and performing a Taylor expansion of the potential energy surface around the equilibrium geometry, they provided expressions for both harmonic and anharmonic contributions to the pure vibrational contributions at different orders. Their analysis in particular demonstrated that the double-harmonic pure vibrational corrections to the hyperpolarizabilities are determined by geometrical gradients of lower-order (hyper)polarizabilities and the dipole moment gradients.

Analytic implementations of dipole moment gradients and polarizability gradients were developed at the Hartree–Fock (HF) level of theory as early as 1992 by Handy and coworkers.[6] However, for the study of pure vibrational hyperpolarizabilities, Quinet and Champagne were the first to present an implementation of frequency-dependent (hyper)polarizability gradients applied to the study of the pure vibrational contributions to the (hyper)polarizabilities.[7,8] Dipole and polarizability gradients have also been implemented for correlated wave functions such as the coupled-cluster wave function.[9] At the density-functional level of theory, van Caillie and Amos presented an analytic implementation of polarizability gradients for the study of Raman intensities,[10] later implemented by Rappaport and Furche using a Lagrangian approach.[11] Coriani *et al.* also presented a linear-scaling formulation of the analytic calculation of polarizability gradients at the density-functional level of theory.[12] A general approach for calculating (hyper)polarizability gradients at the density-functional level of theory formulated in the atomic-orbital basis, and thus amenable for use in linear-scaling formulations of density-functional response theory,[13] has been presented by Thorvaldsen *et al.*,[14] but so far only implemented at the Hartree–Fock level of theory.[15]

The analytic calculations of pure vibrational contributions to the molecular hyperpolarizabilities at the density-functional level of theory are still scant in literature. A recent work by Bulik *et al.*[16] may be the first that calculated the pure vibrational contributions to the first hyperpolarizability analytically. In this paper, we also report the analytic calculations of pure vibrational contributions to the first hyperpolarizability at the density-functional theory (DFT) level. Unlike the study of Bulik *et al.*, our approach follows the formalism of Thorvaldsen *et al.*[14] for evaluating quasi-energy derivatives, using a recursive scheme to generate the response functions to different orders,[17] and using automatic differentiation to generate the exchange-correlation kernels to higher order.[18] Therefore, our developed code (named as OpenRSP) is more general and allows us to calculate the pure vibrational contributions to the molecular (hyper)polarizabilities analytically to arbitrary order. We apply the formalism to calculate the first hyperpolarizabilities (electronic and pure vibrational) for retinal, retinol, retinoic acid, vitamin A acetate, retinal Schiff base (RSB) and protonated retinal Schiff base (PRSB) (see Figure 1 for the molecular structures). We discuss the static dipole hyperpolarizability and the second-harmonic generation (SHG) hyperpolarizability which determines the effects observed in hyper-Rayleigh scattering (HRS) experiments. We present the results for the wavelengths 1064, 1543 and 1907 nm, for which experimental values are available.

Retinal proteins, being biological chromophores, are responsible for light-driven processes in rhodopsin and bacteriorhodopsin. Numerous molecular properties of retinal and related

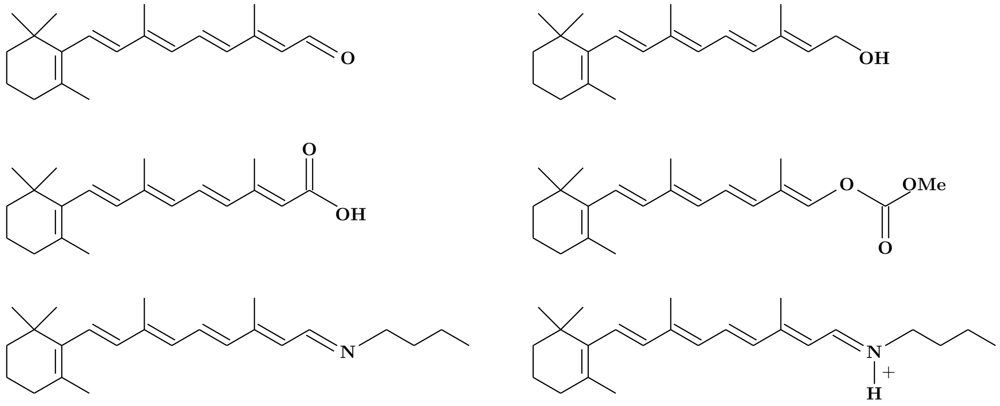

Figure 1: Molecular structures. Top: retinal and retinol; center: retinoic acid and vitamin A acetate; bottom: retinal Schiff base and protonated retinal Schiff base

molecules have been examined in the literature, including second-order optical properties such as the electric dipole hyperpolarizability.[19–21] The frequency-dependent hyperpolarizability of these molecules has been measured applying the hyper-Rayleigh scattering (HRS) technique.[21,22] However, there are significant differences between various experimental data. In particular, the experimental results have been determined with respect to a chosen reference compound, and they depend strongly on the details of the experimental technique used—the values obtained in the internal reference method (IRM) being 4-5 times larger than those obtained in the external reference method (ERM). Moreover, in a specific experiment the results also depend on the chosen solvent—thus, care should be exercised in any comparison with hyperpolarizabilities computed for an isolated molecule. Last but not least, there are no experimental data related to the static hyperpolarizability, the corresponding values determined from experiment represent only the result of an extrapolation. Thus, in addition to presenting a novel implementation of polarizability gradients at the DFT level, our study may help shed light on the accuracy and reliability of the different experimental approaches for determining the first hyperpolarizability.

Theory

The vibrational polarizability and first-order hyperpolarizability are calculated using the perturbation theory approach developed by Bishop and Kirtman.[4,5,23] For completeness, we will here briefly summarize the essential formulas used in our work, highlighting the quantities that we are interested in. We start from the sum-over-states expressions for the (hyper)polarizabilities, for which the polarizability and first-order hyperpolarizability can be written as[4]

$$\alpha_{\alpha\beta}(-\omega_\sigma;\omega_1) = \hbar^{-1}\sum \mathcal{P}_{-\sigma,1}\sum_{k,K}{}^{'}(\omega_{kK}-\omega_\sigma)^{-1} \\ \times \langle 0,0|\hat{\mu}_\alpha|K,k\rangle\langle k,K|\hat{\mu}_\beta|0,0\rangle, \tag{1}$$

$$\beta_{\alpha\beta\gamma}(-\omega_\sigma;\omega_1,\omega_2) = \hbar^{-2}\sum \mathcal{P}_{-\sigma,1,2}\sum_{k,K}{}^{'}\sum_{l,L}{}^{'}(\omega_{kK}-\omega_\sigma)^{-1}(\omega_{lL}-\omega_2)^{-1} \\ \times \langle 0,0|\hat{\mu}_\alpha|K,k\rangle\langle k,K|\overline{\hat{\mu}_\beta}|L,l\rangle\langle l,L|\hat{\mu}_\gamma|0,0\rangle, \tag{2}$$

where $\mathcal{P}_{-\sigma,1(,2)}$ denotes the possible permutations of the electric dipole moment components ($\hat{\mu}_\alpha$, $\hat{\mu}_\beta$, and $\hat{\mu}_\gamma$) and their associated frequencies ($-\omega_\sigma$, ω_1, and ω_2). The capital letters K and L represent the electronic states, whereas k and l refer to the vibrational states. The primes on the summations indicate that we exclude the ground vibronic state $|0,0\rangle$. The energy $\hbar\omega_{kK}$ corresponds to the excitation energy from the ground state to the vibronic state $|K,k\rangle$, and $\overline{\hat{\mu}_\beta} = \hat{\mu}_\beta - \langle 0,0|\hat{\mu}_\beta|0,0\rangle$.

The pure vibrational contributions to the polarizability will be obtained by setting $K = 0$,[4] that is, we only consider excitations within the vibrational manifold

$$\alpha^{\mathrm{v}}_{\alpha\beta}(-\omega_\sigma;\omega_1) = \hbar^{-1}\sum \mathcal{P}_{-\sigma,1}\sum_{k}{}^{'}(\mu_\alpha)_{0k}(\mu_\beta)_{k0}(\omega_k-\omega_\sigma)^{-1} \equiv [\mu^2], \tag{3}$$

where ω_{k0} has been simplified as ω_k and where the notation $(\mu_\alpha)_{0k} \equiv \langle 0|\mu_\alpha^{00}|k\rangle$ is used for the vibrational transition matrix element of the electronic dipole moment $\mu_\alpha^{00} \equiv \langle 0|\hat{\mu}_\alpha|0\rangle$ between the lowest and the k'th vibrational states for the ground electronic state.

The pure vibrational contribution to the hyperpolarizability contains three terms: $(K = 0, L \neq 0)$, $(K \neq 0, L = 0)$, and $(K = 0, L = 0)$[24]

$$\beta^{\mathrm{v}}_{\alpha\beta\gamma}(-\omega_\sigma;\omega_1,\omega_2) \approx \hbar^{-2} \sum \mathcal{P}_{-\sigma,1,2} \left[\sum_k{}' \sum_L{}' \frac{(\mu_\alpha)_{0k}}{\omega_k - \omega_\sigma} \frac{\langle k|\mu_\beta^{0L}\mu_\gamma^{L0}|0\rangle}{\omega_L - \omega_2} \right. \\ \left. + \sum_l{}' \sum_K{}' \frac{(\mu_\alpha)_{l0}}{\omega_l - \omega_2} \frac{\langle 0|\mu_\beta^{0K}\mu_\gamma^{K0}|l\rangle}{\omega_K - \omega_\sigma} + \sum_k{}' \sum_l{}' \frac{(\mu_\alpha)_{0k}}{\omega_k - \omega_\sigma} \frac{(\overline{\mu}_\beta)_{kl}(\mu_\gamma)_{l0}}{\omega_l - \omega_2} \right], \tag{4}$$

where we have used the approximation

$$\omega_{kK} \approx \omega_{0K} \equiv \omega_K (K \neq 0), \quad \omega_{lL} \approx \omega_{0L} \equiv \omega_L (L \neq 0), \tag{5}$$

and the notation $\mu_\alpha^{KL} \equiv \langle K|\hat{\mu}_\alpha|L\rangle$ accounts for the electronic transition moment between the electronic states K and L.

The third term in $\beta^{\mathrm{v}}_{\alpha\beta\gamma}(-\omega_\sigma;\omega_1,\omega_2)$ is often denoted $[\mu^3]$, and the sum of the first and second terms is the so-called $[\mu\alpha]$ contribution,[23] which becomes

$$[\mu\alpha] \approx \frac{1}{2}\hbar^{-1} \sum \mathcal{P}_{-\sigma,1,2} \sum_k{}' (\mu_\alpha^{00})_{0k} (\alpha_{\beta\gamma}^{00})_{k0} (\omega_k \pm \omega_\sigma)^{-1}, \tag{6}$$

when the applied frequencies and their combinations are far away from electronic resonances and we can apply the approximation $(\omega_i = \omega_\sigma, \omega_1, \omega_2)$[4]

$$\omega_K, \omega_L \gg \omega_i \Rightarrow \begin{cases} \omega_K \pm \omega_i \approx \omega_K \\ \omega_L \pm \omega_i \approx \omega_L \end{cases} \quad (K, L \neq 0). \tag{7}$$

In Eq. (6), we have also introduced[4]

$$(\omega_k \pm \omega_\sigma)^{-1} = (\omega_k + \omega_\sigma)^{-1} + (\omega_k - \omega_\sigma)^{-1}, \tag{8}$$

$$(\alpha_{\beta\gamma})_{k0} = \langle k|\alpha^{00}_{\beta\gamma}|0\rangle, \tag{9}$$

with

$$\alpha^{00}_{\beta\gamma} = 2\hbar^{-1}\sum_L{}' \frac{\mu^{0L}_\beta \mu^{L0}_\gamma}{\omega_L} \tag{10}$$

being the static electronic polarizability.

The vibrational transition matrix elements, such as $(\mu_\alpha)_{0k}$ and $(\alpha_{\beta\gamma})_{k0}$ defined in the aforementioned equations, can be calculated by expanding the electronic dipole moment, polarizability, and vibrational potential in displacements along the normal coordinates (q_v) around the equilibrium geometry.[4,23] In the double-harmonic approximation, only $[\mu^2]$ and $[\mu\alpha]$ contribute to the polarizability and the first-order hyperpolarizability, respectively,[4,23] with

$$\alpha^{\mathrm{v}}_{\alpha\beta}(-\omega_\sigma;\omega_1) \approx \left[\mu^2\right]^{(0,0)} = \frac{1}{2}\sum \mathcal{P}_{-\sigma,1}\sum_v \frac{\partial\mu_\alpha}{\partial q_v}\frac{\partial\mu_\beta}{\partial q_v}\lambda^{\pm\sigma}_v, \tag{11}$$

$$\beta^{\mathrm{v}}_{\alpha\beta\gamma}(-\omega_\sigma;\omega_1,\omega_2) \approx \left[\mu\alpha\right]^{(0,0)} = \frac{1}{2}\sum \mathcal{P}_{-\sigma,1,2}\sum_v \frac{\partial\mu_\alpha}{\partial q_v}\frac{\partial\alpha_{\beta\gamma}}{\partial q_v}\lambda^{\pm\sigma}_v, \tag{12}$$

where the frequency terms are defined as

$$\lambda^{\pm\sigma}_v = \left(\omega^2_v - \omega^2_\sigma\right)^{-1}. \tag{13}$$

The evaluation of $[\mu^2]^{(0,0)}$ and $[\mu\alpha]^{(0,0)}$ using our recently developed atomic-orbital based quasienergy formalism[14] has been discussed in Ref. 15 in the case of Hartree–Fock wave functions, in which a static field (that is, with a zero frequency) has been employed. In the case of dynamic fields, as shown in Eqs. (11) and (12), the frequency of the external field only enters the terms $\lambda^{\pm\sigma}_v$. The evaluation of the geometric derivatives of polarizabilities and hyperpolarizabilities hence follow the same procedure as in the static case—being obtained as the derivatives of the quasienergy Q.[14] Here we extend our implementation of the dipole and polarizability gradients to the density-functional level of theory.

At the DFT level, with an externally applied electric field $\vec{F}$, the derivative of Q with respect to a displacement q_v (the gradient) is given by

$$\begin{aligned}\frac{\mathrm{d}Q}{\mathrm{d}q_v} &= \frac{\partial}{\partial q_v}\Big(h_{\mathrm{nuc}} - \vec{F}\cdot\vec{\mu}_{\mathrm{nuc}} + \mathrm{Tr}\Big[\mathbf{h} - \vec{F}\cdot\vec{\boldsymbol{\mu}} + \tfrac{1}{2}\mathbf{G}^{\gamma}(\mathbf{D}) + \mathbf{F}_{\mathrm{xc}}\Big]\mathbf{D}\Big) - \mathrm{Tr}\frac{\partial \mathbf{S}}{\partial q_v}\mathbf{W} \\ &= h^{v}_{\mathrm{nuc}} - \vec{F}\cdot\vec{\mu}^{v}_{\mathrm{nuc}} + \mathrm{Tr}\Big[\mathbf{h}^{v} - \vec{F}\cdot\vec{\boldsymbol{\mu}}^{v} + \tfrac{1}{2}\mathbf{G}^{\gamma,v}(\mathbf{D}) + \mathbf{F}^{v}_{\mathrm{xc}}\Big]\mathbf{D} - \mathrm{Tr}\,\mathbf{S}^{v}\mathbf{W},\end{aligned} \tag{14}$$

where h_{nuc} is the nuclear repulsion energy, $-\vec{F}\cdot\vec{\mu}_{\mathrm{nuc}}$ is the interaction energy obtained from the interaction of the external field with the nuclei, $\mathbf{h}$ is the one-electron Hamiltonian (kinetic energy and nuclear attraction) integral matrix, $-\vec{F}\cdot\vec{\boldsymbol{\mu}}$ are the electron–electric field (dipole) interaction integrals, $\mathbf{G}$ is the two-electron (Coulomb and [γ fractional] exchange) integral tensor $\mathbf{G}^{\gamma}_{\kappa\lambda}(\mathbf{D}) = \sum_{\mu\nu}\mathbf{D}_{\nu\mu}(g_{\kappa\lambda\mu\nu} - \gamma g_{\kappa\nu\mu\lambda})$ with the two-electron integral $g_{\kappa\lambda\mu\nu} = \iint \chi^{*}_{\kappa}(\mathbf{r}_1)\chi_{\lambda}(\mathbf{r}_1)\frac{1}{r_{12}}\chi^{*}_{\mu}(\mathbf{r}_2)\chi_{\nu}(\mathbf{r}_2)\mathrm{d}\mathbf{r}_1\mathrm{d}\mathbf{r}_2$ over basis functions χ's, $\mathbf{D}$ is the atomic orbital (AO) density matrix (dependent variable), and $\mathbf{S}$ is the AO overlap matrix, and where we have also introduced a superscript notation for the differentiated quantities.

$\mathbf{W}$ in Eq. (14) is the so-called "energy-weighted density matrix",[14] given by the formula

$$\mathbf{W} = \mathbf{D}\Big[\mathbf{h} - \vec{F}\cdot\vec{\boldsymbol{\mu}} + \mathbf{G}^{\gamma}(\mathbf{D}) + \mathbf{F}_{\mathrm{xc}}\Big]\mathbf{D} + \frac{\mathrm{i}}{2}\frac{\partial \mathbf{D}}{\partial t}\mathbf{S}\mathbf{D} - \frac{\mathrm{i}}{2}\mathbf{D}\mathbf{S}\frac{\partial \mathbf{D}}{\partial t}. \tag{15}$$

We note that although the two last terms vanish for the (time-independent) unperturbed state, perturbation by a time-dependent $\vec{F}$ will induce a time-dependent perturbed $\mathbf{D}$, and thus nonzero contributions to the perturbed $\mathbf{W}$.

$\mathbf{F}_{\mathrm{xc}}$ in Eq. (14) is the exchange–correlation (XC) potential matrix, defined within the adiabatic approximation as[14]

$$(F_{\mathrm{xc}})_{\kappa\lambda} = \int \mathrm{d}\mathbf{r}\ \Omega_{\kappa\lambda}(\mathbf{r}) v_{\mathrm{xc}}(\mathbf{r}), \tag{16}$$

where $\Omega_{\kappa\lambda}(\mathbf{r})$ is the overlap distribution of the basis functions χ_κ and χ_λ

$$\Omega_{\kappa\lambda}(\mathbf{r}) = \chi_\kappa^*(\mathbf{r}) \chi_\lambda(\mathbf{r}), \tag{17}$$

and $v_{\mathrm{xc}}(\mathbf{r})$ is the XC potential defined as the functional derivative of the XC energy E_{xc} with respect to the density $n(\mathbf{r})$

$$v_{\mathrm{xc}}(\mathbf{r}) = \frac{\delta E_{\mathrm{xc}}}{\delta n(\mathbf{r})}. \tag{18}$$

In this work we employ an XC energy E_{xc} defined as the integral over a local function $\epsilon_{\mathrm{xc}}(\mathbf{r})$ that depends on the density $n(\mathbf{r})$ and its Cartesian gradient $\nabla n(\mathbf{r})$

$$E_{\mathrm{xc}}(\mathbf{r}) = \int \mathrm{d}\mathbf{r}\ \epsilon_{\mathrm{xc}}(n(\mathbf{r}), \nabla n(\mathbf{r})). \tag{19}$$

The XC energy and the XC potential matrix are integrated on a numerical grid defined by a set of suitably chosen grid points $\mathbf{r}_i$ and grid weights w_i, according to

$$E_{\mathrm{xc}} \approx \sum_i w_i \epsilon_{\mathrm{xc}}(\mathbf{r}_i). \tag{20}$$

$$(F_{\mathrm{xc}})_{\kappa\lambda} \approx \sum_i w_i \Omega_{\kappa\lambda}(\mathbf{r}_i) v_{\mathrm{xc}}(\mathbf{r}_i). \tag{21}$$

In this work we use a standard grid and when differentiating the XC energy and the XC potential matrix we ignore the contribution from the grid-weight derivatives. This approximation has been validated by comparison with finite difference results.

Formulas for the electric dipole and polarizability gradients are obtained by differentiating the gradient in Eq. (14) once and twice, respectively, with respect to $\vec{F}$, while taking the dependence of $\mathbf{D}$ on $\vec{F}$ into account, and evaluating the resulting equations at $\vec{F} = 0$[15]

$$
\begin{aligned}
-\frac{\partial \mu_\alpha}{\partial q_v} =& \frac{\mathrm{d}^2 Q}{\mathrm{d}q_v \mathrm{d}F_\alpha} = -\mu^v_{\mathrm{nuc},\alpha} - \mathrm{Tr}\, \boldsymbol{\mu}^v_\alpha \mathbf{D} \qquad (22)\\
&+ \mathrm{Tr}\big[\mathbf{h}^v + \mathbf{G}^{\gamma,v}(\mathbf{D})\big]\mathbf{D}^\alpha + E^{v\alpha}_{\mathrm{xc}} - \mathrm{Tr}\,\mathbf{S}^v \mathbf{W}^\alpha,\\
-\frac{\partial \alpha_{\alpha\beta}}{\partial q_v} =& \frac{\mathrm{d}^3 Q}{\mathrm{d}q_v \mathrm{d}F_\alpha \mathrm{d}F_\beta} = -\mathrm{Tr}\, \boldsymbol{\mu}^v_\alpha \mathbf{D}^\beta - \mathrm{Tr}\, \boldsymbol{\mu}^v_\beta \mathbf{D}^\alpha \qquad (23)\\
&+ \mathrm{Tr}\big[\mathbf{h}^v + \mathbf{G}^{\gamma,v}(\mathbf{D})\big]\mathbf{D}^{\alpha\beta} + \mathrm{Tr}\,\mathbf{G}^{\gamma,v}(\mathbf{D}^\beta)\mathbf{D}^\alpha + E^{v\alpha\beta}_{\mathrm{xc}} - \mathrm{Tr}\,\mathbf{S}^v \mathbf{W}^{\alpha\beta}.
\end{aligned}
$$

We note that these gradients are evaluated in Cartesian nuclear coordinates, and then transformed to normal coordinates for the vibrational analysis.

Let us briefly comment on the evaluation of the XC contributions $E^{v\alpha}_{\mathrm{xc}}$ and $E^{v\alpha\beta}_{\mathrm{xc}}$. Ignoring grid-weight derivatives, we can focus on the computation of the XC energy density derivatives $\epsilon^{v\alpha}_{\mathrm{xc}}(\mathbf{r})$ and $\epsilon^{v\alpha\beta}_{\mathrm{xc}}(\mathbf{r})$ (see Eq. (20)). To evaluate these XC energy density derivatives, we first compute the unperturbed densities $n(\mathbf{r})$ and density gradients $\nabla n(\mathbf{r})$ and their derivatives with respect to the applied perturbations $n^v(\mathbf{r}), n^{(\alpha)}(\mathbf{r}), n^{v(\alpha)}(\mathbf{r}), n^{(\beta)}(\mathbf{r}), n^{v(\beta)}(\mathbf{r}), n^{(\alpha\beta)}(\mathbf{r}), n^{v(\alpha\beta)}(\mathbf{r})$ and their Cartesian gradients according to

$$n^{(p)}(\mathbf{r}) = \sum_{\kappa\lambda} \Omega_{\kappa\lambda}(\mathbf{r}) D^p_{\lambda\kappa} \qquad (24)$$

$$\nabla n^{(p)}(\mathbf{r}) = \sum_{\kappa\lambda} \nabla\Omega_{\kappa\lambda}(\mathbf{r}) D^p_{\lambda\kappa} \qquad (25)$$

$$n^{v(p)}(\mathbf{r}) = \sum_{\kappa\lambda} \Omega^v_{\kappa\lambda}(\mathbf{r}) D^p_{\lambda\kappa} \qquad (26)$$

$$\nabla n^{v(p)}(\mathbf{r}) = \sum_{\kappa\lambda} \nabla\Omega^v_{\kappa\lambda}(\mathbf{r}) D^p_{\lambda\kappa} \qquad (27)$$

In this work we do not form $\epsilon^{v\alpha}_{\mathrm{xc}}(\mathbf{r})$ and $\epsilon^{v\alpha\beta}_{\mathrm{xc}}(\mathbf{r})$ by explicitly applying the chain rule using XC functional derivatives and the above perturbed densities. Instead, we evaluate $\epsilon^{v\alpha}_{\mathrm{xc}}(\mathbf{r})$ and $\epsilon^{v\alpha\beta}_{\mathrm{xc}}(\mathbf{r})$ directly by calling the XCFun library[18,25] with appropriate density (gradient) perturbation expansions $[n, n^v, n^{(\alpha)}, n^{v(\alpha)}]$ and $[n, n^v, n^{(\alpha)}, n^{v(\alpha)}, n^{(\beta)}, n^{v(\beta)}, n^{(\alpha\beta)}, n^{v(\alpha\beta)}]$, respectively. This scheme is easily extensible to higher orders and to XC functionals that depend on additional density variables.

The electronic polarizability $\alpha_{\alpha\beta}(-\omega_\sigma;\omega_1)$ and first-order hyperpolarizability $\beta_{\alpha\beta\gamma}(-\omega_\sigma;\omega_1,\omega_2)$ are also derivatives of the quasienergy and given by

$$-\alpha_{\alpha\beta} = \frac{\mathrm{d}^2 Q}{\mathrm{d}F_\alpha \mathrm{d}F_\beta} = -\mathrm{Tr}\,\boldsymbol{\mu}_\beta \mathbf{D}^\alpha, \tag{28}$$

$$-\beta_{\alpha\beta\gamma} = \frac{\mathrm{d}^3 Q}{\mathrm{d}F_\alpha \mathrm{d}F_\beta \mathrm{d}F_\gamma} = -\mathrm{Tr}\,\boldsymbol{\mu}_\gamma \mathbf{D}^{\alpha\beta}. \tag{29}$$

Although of the same order as the gradients in Eqs. (22)–(23), these formulas are much simpler because the AOs do not depend on $\vec{F}$, whereas they do depend on q_v.

The first- and second-order perturbed density matrices in Eqs. (22)–(29), $\mathbf{D}^\alpha$ and $\mathbf{D}^{\alpha\beta}$, respectively, can be obtained from a set of linear equations of the same form,[14] allowing us to use the same solver for both equations. In this work, we will use the conventional molecular orbital-based response solver of the DALTON program,[26] thus the right-hand sides that enter into the linear response equations are transformed from AO to the molecular orbital (MO) basis, and the resulting response vectors backtransformed from the MO to AO basis, in a manner similar to that previously used in four-component relativistic calculations of nonlinear optical properties.[27]

Results

The results will be reported for the isotropic averages, defined by the equations

$$\alpha = \frac{1}{3}\sum_\eta \alpha_{\eta\eta}, \tag{30}$$

$$\beta_Z = \frac{1}{5}\sum_\eta (\beta_{Z\eta\eta} + \beta_{\eta Z\eta} + \beta_{\eta\eta Z}) \tag{31}$$

where $\eta = x, y, z$ and the Z axis is determined by the direction of the dipole moment (we note that this definition of the hyperpolarizability includes its sign, not determined in experiment[22]). We shall discuss only the static hyperpolarizability and the second-harmonic generation process $\beta^{\text{SHG}} = \beta(-2\omega; \omega, \omega)$. Our discussion of correlation effects will focus on these effects on the pure vibrational contributions as described by DFT using the Becke's three-parameter exchange functional[28] and the Lee–Yang–Parr (LYP) correlation functional[29] in the form of the B3LYP functional,[30] as correlation effects as described by DFT on the electronic hyperpolarizabilities have already been discussed in a number of different studies.[31–35]

We have optimised molecular geometries for the *all-trans* structures, using the B3LYP functional and the Turbomole-TZV2P basis set,[36] and at this computational level we have also determined the molecular Hessian, used in the analysis of the vibrational (hyper)polarizabilities. The calculation of electronic and pure vibrational contributions to the (hyper)polarizabilities have been calculated using the Sadlej-pVTZ[37] basis set at the Hartree–Fock and density functional level of theory using the B3LYP functional.

Polarizability

Electronic and vibrational contributions to the dipole polarizability are shown in Table 1. We observe smooth frequency dependence of the electronic polarizability, encompassing the static values, for all the molecules, with the dispersion effects noticeably larger for the protonated retinal Schiff base than for the other molecules. The B3LYP results are in the static case about 12–14% larger than the Hartree–Fock results, independently of the molecule. For the frequency-dependent electronic polarizabilities, the effect of electron correlation increases somewhat and in particular gives larger differences between the different molecules, in general being about $16 - 22\%$ of the Hartree–Fock values at a wavelength of 771 nm. An exception to this rule is the protonated retinal Schiff base, which has a correlation effect of almost 33% at 771 nm. These differences are due to the differences in the pole structure, DFT correcting (possibly overcorrecting) the well-known overestimation of the HOMO–LUMO (the highest occupied and lowest unoccupied molecular orbitals) gap by Hartree–Fock. We note that in the case of the protonated retinal Schiff base, the lowest excitation wavelength is only slightly longer than 532 nm, explaining the change in sign and large magnitude of the electronic polarizability of this molecule at 532 nm.

The vibrational contributions are practically negligible in the range of frequencies studied. On the other hand, for the static polarizabilities they are of the same order of magnitude as the electronic terms (in the case of vitamin A acetate, the vibrational contribution actually dominates). The larger vibrational contributions for the static polarizabilities can be understood from Eq. (11) observing that the frequency of the external field only enters the terms $\lambda_v^{\pm\sigma}$, and we have for each mode v the ratio of $\lambda_v^{\pm\sigma}$ between the dynamic and static polarizabilities as $\frac{\lambda_v^{\pm\sigma}(\omega)}{\lambda_v^{\pm\sigma}(0)} = -\frac{\omega_v^2}{\omega^2-\omega_v^2} \approx -\frac{\omega_v^2}{\omega^2}$.[38] Here we have used the fact that the frequency ω in our studies is usually larger than that of the vibrational mode v. Therefore, the vibrational contributions for the dynamic polarizabilities are generally one to three order of magnitude smaller than those for the static polarizabilities in our studies, and also have a change of sign as clearly shown in Table 1. Another important observation is that in most cases B3LYP gives only a slightly smaller pure vibrational polarizability than Hartree–Fock for retinal, retinoic acid and retinal Schiff base. In contrast, for retinol, vitamin A acetate and protonated retinal Schiff base, B3LYP reduces the magnitude of the pure vibrational corrections to the static polarizability by a factor of 2–3, despite the very minor differences in the structure compared to the three other molecules.

First hyperpolarizability

We will discuss the electronic and vibrational contributions to the first hyperpolarizability collected in Table 2 and compare them to available experimental data. As for the polarizabilities, the vibrational contributions at the frequencies of interest are practically negligible for the SHG process, and we thus begin the discussion and comparison with experiment focusing on the electronic contributions.

Table 1: Electric dipole polarizabilities (in 10^{-25} esu)

wavelength nm	retinal	retinol	retinoic acid	vitamin A acetate	retinal Schiff base	protonated RSB
electronic, HF						
532	558.90	507.79	547.52	541.81	686.64	1420.28
771	497.37	466.93	492.35	498.87	612.81	865.69
953	483.15	456.85	479.36	488.27	595.71	794.54
1064	478.27	453.33	474.89	484.58	589.84	772.79
1543	468.53	446.22	465.93	477.10	578.12	732.68
1907	465.65	444.10	463.28	474.87	574.66	721.63
∞	460.40	440.19	458.42	470.77	568.33	702.31
vibrational, HF						
532	−0.17	−0.08	−0.20	−0.23	−0.12	−1.76
771	−0.36	−0.18	−0.43	−0.48	−0.25	−3.73
953	−0.56	−0.28	−0.67	−0.74	−0.39	−5.73
1064	−0.71	−0.35	−0.84	−0.93	−0.49	−7.18
1543	−1.57	−0.80	−1.88	−2.05	−1.13	−15.55
1907	−2.57	−1.35	−3.09	−3.32	−1.92	−24.55
∞	156.57	355.29	132.06	789.30	80.83	492.34
electronic, DFT						
532	809.45	634.85	763.57	696.23	964.09	−8552.58
771	603.95	540.48	593.33	589.25	741.08	1151.73
953	571.16	521.23	564.29	567.64	703.24	975.43
1064	560.72	514.81	554.93	560.45	691.08	929.39
1543	540.92	502.23	537.04	546.39	667.86	852.06
1907	535.33	498.58	531.96	542.32	661.27	832.25
∞	525.41	492.00	522.90	534.98	649.54	798.99
vibrational, DFT						
532	−0.15	−0.074	−0.17	−0.20	−0.10	−0.69
771	−0.31	−0.154	−0.36	−0.42	−0.21	−1.45
953	−0.48	−0.244	−0.56	−0.66	−0.32	−2.24
1064	−0.61	−0.304	−0.70	−0.82	−0.41	−2.80
1543	−1.35	−0.684	−1.55	−1.81	−0.93	−6.09
1907	−2.20	−1.154	−2.54	−2.92	−1.58	−9.66
∞	132.73	117.714	111.13	326.08	67.75	256.99

Table 2: SHG hyperpolarizabilities (in 10^{-30} esu)

wavelength nm	retinal	retinol	retinoic acid	vitamin A acetate	retinal Schiff base	protonated RSB
electronic, HF						
1064	40.99	−2.20	32.76	−1.07	14.17	−601.59
1543	27.07	−1.46	21.99	−1.32	8.67	−223.57
1907	24.10	−1.30	19.65	−1.37	7.53	−179.04
∞	19.58	−1.05	16.07	−1.41	5.81	−124.46
vibrational, HF						
1064	−1.05	−0.00	−0.86	0.09	−0.47	9.72
1543	−2.25	−0.01	−1.83	0.19	−1.01	20.89
1907	−3.51	−0.01	−2.83	0.31	−1.59	32.65
∞	168.37	88.45	136.01	149.03	61.16	−805.60
electronic, DFT						
1064	250.17	−18.97	190.99	20.32	116.65	6542.78
1543	101.32	−9.34	83.44	8.05	45.52	−305.43
1907	81.71	−7.74	68.17	6.13	35.94	−204.25
∞	57.15	−5.60	48.58	3.64	24.03	−113.36
vibrational, DFT						
1064	−1.07	0.03	−0.91	0.09	−0.59	2.30
1543	−2.30	0.06	−1.95	0.20	−1.27	4.93
1907	−3.59	0.09	−3.01	0.32	−1.99	7.68
∞	187.76	−26.34	142.64	105.85	87.30	−213.31
experimental, IRM, in methanol[22]						
1064	730	–	310	140	470	3600
experimental, ERM, in methanol[21]						
1064	133	18	60	37	116	1095
experimental, IRM, in chloroform[22]						
1064	270	–	110	–	–	–
experimental, ERM, in chloroform[21]						
1064	111	12	44	31	–	–
1543	49	10	33	13	–	–
1907	11	8	14	9	–	–
from experimental data, IRM, in methanol[22]						
∞	300	–	160	80	220	900
from experimental data, ERM in methanol[21]						
∞	57	10	30	20	54	271
INDO/SOS[22]						
∞	41.5	–	38.0	2.4	17.9	214.6

Electronic hyperpolarizabilities

As already mentioned, the experimental data are obtained with respect to a reference compound, and the absolute values of the hyperpolarizabilities are not really known. Another comparison of the computed and measured quantities is thus given in Table 3, where all the static hyperpolarizabilities have been defined with respect to the corresponding retinal value.

Table 3: Rescaled SHG electronic hyperpolarizabilities[a]

wavelength nm	retinal	retinol	retinoic acid	vitamin A acetate	retinal Schiff base	protonated RSB
This work, HF						
∞	1.00	−0.05	0.82	−0.07	0.30	−6.36
This work, DFT						
∞	1.00	−0.10	0.85	0.06	0.42	−1.98
from experimental data, ERM in methanol[21]						
∞	1.00	0.18	0.53	0.35	0.95	4.75
from experimental data, extrapolated[22]						
∞	1.00	–	0.53	0.27	0.73	3.00
INDO/SOS[22]						
∞	1.00	–	0.92	0.06	0.43	5.17
Frequency dispersion						
This work, HF						
1064	2.093	2.089	2.039	0.757	2.437	4.834
This work, DFT						
1064	4.377	3.389	3.931	5.585	4.855	−57.716
experimental, IRM, in methanol[22]						
1064	2.433	–	1.938	1.750	2.136	4.000
experimental, ERM, in methanol[21]						
1064	2.333	1.800	2.000	1.850	2.148	4.041

[a] All the static hyperpolarizabilities are defined with respect to the analogous static retinal values, all the dynamic hyperpolarizabilities with respect to the corresponding static values of the same molecule.

The ordering of the β(electronic) magnitudes in experiment[21] is

PRSB $>$ retinal $>$ RSB $>$ retinoic acid $>$ vitamin A acetate $>$ retinol

with the same ordering as in Ref. 22, as well as for the values extrapolated to zero frequency, and

PRSB > retinal > retinoic acid > RSB > retinol > vitamin A acetate

in our calculations at the B3LYP level of theory. This ordering is confirmed by the Hartree–Fock calculations with the exception of the two molecules with the smallest hyperpolarizability, retinol and vitamin A acetate, which switch order in the Hartree–Fock calculations compared to B3LYP. Our results indicate, similarly to the INDO/SOS calculations, that the hyperpolarizability of retinoic acid is larger than that of RSB, in contrast to the experimental ordering. As noticed in Ref. 22, there is no obvious explanation for this disagreement with experimental data. The somewhat stronger increase in the rescaled electronic hyperpolarizabilities obtained at 1064 nm compared to the static limit reflects the fact that HF in general overestimates the excitation energies whereas DFT underestimates the excitation energies. The fact that HF agrees better with experiment at 1064 nm than DFT may suggest that we are seeing indications of the well-known DFT catastrophe for long, conjugated systems.[39]

Electron correlation effects as described by the B3LYP functional are in general much larger for the first hyperpolarizability than for the polarizability, also for the static value, the B3LYP hyperpolarizability being in general 2.5–5 times larger than at the Hartree–Fock level of theory. Interestingly, the exception to this rule is the protonated retinal Schiff base, where B3LYP actually gives a smaller value for the hyperpolarizability than Hartree–Fock. Including frequencies, the differences between Hartree–Fock and B3LYP increase, at 1064 nm the B3LYP results being in general 6–8 times larger than Hartree–Fock, with the exceptional case being the vitamin A acetate where the B3LYP first hyperpolarizability not only is 20 times larger than at the Hartree–Fock level of theory, but also has the opposite sign. For this molecule, there is a delicate interplay between the contributing channels to the calculated electronic hyperpolarizability. The results for the protonated retinal Schiff base at 1064 nm is once again a consequence of the near-resonance conditions at 2ω.

Vibrational hyperpolarizabilities

The vibrational contributions to the first hyperpolarizability, shown in Table 2, are somewhat more important than the corresponding contributions to the polarizability. They vary smoothly with the frequency and at 1907 nm reach ≈20% of the electronic contribution (with, for most molecules, opposite sign). In principle, the experimental values represent the total hyperpolarizability. However, considering all the difficulties in determing the absolute value of the hyperpolarizability from experiment, the role of the solvent, and all the approximations made in the theory for extracting the hyperpolarizabilities from the experimental measurements, it is practically impossible to obtain from the comparison of computed and measured values any information on the vibrational terms.

On the other hand, the vibrational contribution to the static hyperpolarizabilities is very large. Whereas for the polarizability it was of a similar magnitude as the electronic term, for the hyperpolarizability it is clearly dominant for each molecule. In this case, the electronic terms are almost negligible, but—as discussed above—there are no experimental data for the total static hyperpolarizabilities, the extrapolation from frequency-dependent values yields only the electronic part.

We note that whereas the pure vibrational contribution to the polarizability by necessity of its form (see Eq. (11)) has to have the same sign at any optical frequency (since these are larger than the vibrational frequency), the pure vibrational contribution to the first hyperpolarizability can be of either sign. This is also reflected in the calculated pure vibrational contributions where no clear trends can be observed, which is surprising considering the very close structural features of the molecules investigated. We note in particular that for both the static and the frequency-dependent pure vibrational contribution to retinol, a change of sign is observed when going from Hartree–Fock to B3LYP. The protonated Schiff base also displays very large electron correlation effects on the pure vibrational contribution to the static first hyperpolarizability, reducing the Hartree–Fock value by almost a factor of four. These results illustrate that it in general can be difficult to predict the effects of electron correlation on the pure vibrational contributions, even for a class of structurally related molecules. Explicit calculations including electron correlation effects, such as DFT, is therefore advisable. The analytic scheme presented here allows such calculations to be efficiently performed also for large molecules at the density-functional level of theory.

Conclusions

We have presented an analytic implementation of pure vibrational contributions to the polarizability and first hyperpolarizability at the density functional level of theory. The approach is based on a recursive implementation of a density-matrix-based approach for calculating higher-order molecular properties, using automatic differentiation to evaluate the exchange–correlation kernels.

We have studied the electronic and vibrational contributions to the first dipole hyperpolarizabilities of retinal and related molecules. The frequency-dependent first hyperpolarizability, which determines the second-harmonic generation, is dominated by the electronic terms. The absolute values of the hyperpolarizabilities are difficult to determine from experimental data, but their relative values obtained from the calculations are in reasonable agreement with experiment. In particular, the value computed for the protonated retinal Schiff base is—in agreement with experiment—significantly larger than for any other molecule considered (the dispersion effects are also the largest for PRSB). We note, however, that the computed hyperpolarizabilities are in better agreement with previously published semi-empirical results than with experimental data, and the previously observed differences with respect to experiment are not removed in the approach we have used.

In the analysis of static hyperpolarizabilities it is essential to include the vibrational contributions. These terms do not significantly affect the SHG values or the dispersion at frequencies of experimental interest, but the extrapolation to zero frequency of the measured optical hyperpolarizabilities provides only an estimate of the corresponding electronic contribution. For the static dipole hyperpolarizability, as is well known and also shown by the calculations, the vibrational contribution may be equally important to or even larger than the electronic term. We have demonstrated that the electron correlation effects vary significantly for the pure vibrational corrections to the static first hyperpolarizability, illustrating the need for analytic schemes for (hyper)polarizability derivatives at the DFT level of theory.

Acknowledgement

This work has received support from the European Research Council through a Starting Grant to K.R. (Grant No. 279619), the Research Council of Norway through a Centre of Excellence Grant (Grant No. 179568/V30) and Grant No. 191251/V30. A grant of computer time from the Programme for Supercomputing is also gratefully acknowledged (Grant No. NN4654K).

References

(1) Bishop, D. M. Molecular Vibrational and Rotational Motion in Static and Dynamic Electric Fields. *Rev. Mod. Phys.* **1990**, *62*, 343–374.

(2) Champagne, B.; Legrand, T.; Perpete, E. A.; Quinet, O.; André, J. M. Ab Initio Hartree-Fock Investigation of π-Conjugated Compounds Presenting Large β^v/β^e Ratio: Merocyanines. *Coll. Czech Chem. Comm.* **1998**, *63*, 1295–1308.

(3) Kirtman, B.; Champagne, B.; Luis, J. M. Efficient Treatment of the Effect of Vibrations on Electrical, Magnetic, and Spectroscopic Properties. *J. Comput. Chem.* **2000**, *21*, 1572–1588.

(4) Bishop, D. M.; Kirtman, B. A Perturbation Method for Calculating Vibrational Dynamic Dipole Polarizabilities and Hyperpolarizabilities. *J. Chem. Phys.* **1991**, *95*, 2646–2658.

(5) Bishop, D. M.; Kirtman, B. Compact Formulas for Vibrational Dynamic Dipole Polarizabilities and Hyperpolarizabilities. *J. Chem. Phys.* **1992**, *97*, 5255–5256.

(6) Jayatilaka, D.; Maslen, P. E.; Amos, R. D.; Handy, N. C. Higher Analytic Derivatives. III. Geometrical Derivatives of the Dipole and Dipole Polarizabilities. *Mol. Phys.* **1992**, *75*, 271–291.

(7) Quinet, O.; Champagne, B. Time-Dependent Hartree–Fock Schemes for Analytical Evaluation of the Raman Intensities. *J. Chem. Phys.* **2001**, *115*, 6293–6299.

(8) Quinet, O.; Champagne, B. Analytical Time-Dependent Hartree–Fock Schemes for the Evaluation of the Hyper-Raman Intensities. *J. Chem. Phys.* **2002**, *117*, 2481–2488.

(9) O'Neill, D. P.; Kállay, M.; Gauss, J. Calculation of Frequency-Dependent Hyperpolarizabilities Using General Coupled-Cluster Models. *J. Chem. Phys.* **2007**, *127*, 134109.

(10) Caillie, C. V.; Amos, R. D. Raman Intensities Using Time Dependent Density Functional Theory. *Phys. Chem. Chem. Phys.* **2000**, *2*, 2123–2129.

(11) Rappoport, D.; Furche, F. Lagrangian Approach to Molecular Vibrational Raman Intensities Using Time-Dependent Hybrid Density Functional Theory. *J. Chem. Phys.* **2007**, *126*, 201104.

(12) Coriani, S.; Kjærgaard, T.; Jørgensen, P.; Ruud, K.; Huh, J.; Berger, R. An Atomic-Orbital-Based Lagrangian Approach for Calculating Geometric Gradients of Linear Response Properties. *J. Chem. Theory Comput.* **2010**, *6*, 1028–1047.

(13) Coriani, S.; Høst, S.; Jansik, B.; Thøgersen, L.; Olsen, J.; Jørgensen, P.; Reine, S.; Pawlowski, F.; Helgaker, T.; Sałek, P. Linear-Scaling Implementation of Molecular Response Theory in Self-Consistent Field Electronic-Structure Theory. *J. Chem. Phys.* **2007**, *126*, 154108.

(14) Thorvaldsen, A. J.; Ruud, K.; Kristensen, K.; Jørgensen, P.; Coriani, S. A Density Matrix-Based Quasienergy Formulation of the Kohn–Sham Density Functional Response Theory Using Perturbation- and Time-Dependent Basis Sets. *J. Chem. Phys.* **2008**, *129*, 214108.

(15) Thorvaldsen, A. J.; Ruud, K.; Jaszuński, M. Analytic Calculations of Vibrational Hyperpolarizabilities in the Atomic Orbital Basis. *J. Phys. Chem. A* **2008**, *112*, 11942–11950.

(16) Bulik, I. W.; Zaleśny, R.; Bartkowiak, W.; Luis, J. M.; Kirtman, B.; Scuseria, G. E.; Avramopoulos, A.; Reis, H.; Papadopoulos, M. G. Performance of Density Functional Theory in Computing Nonresonant Vibrational (Hyper)polarizabilities. *J. Comput. Chem.* **2013**, *34*, 1775–1784.

(17) Ringholm, M.; Jonsson, D.; Ruud, K. A General, Recursive and Open-Ended Response Code. *J. Comput. Chem.* **2013**, accepted.

(18) Ekström, U.; Visscher, L.; Bast, R.; Thorvaldsen, A. J.; Ruud, K. Arbitrary-Order Density Functional Response Theory from Automatic Differentiation. *J. Chem. Theory Comput.* **2010**, *6*, 1971–1980.

(19) Kawabe, Y.; Ikeda, H.; Sakai, T.; Kawasaki, K. Second-Order Non-Linear Optical Properties of New Organic Conjugated Molecules. *J. Mat. Chem.* **1992**, *2*, 1025–1031.

(20) Clays, K.; Van Elshocht, S.; Chi, M. J.; Lepoudre, E.; Persoons, A. Bacteriorhodopsin: A Natural, Efficient (Nonlinear) Photonic Crystal. *J. Opt. Soc. Am. B* **2001**, *18*, 1474–1482.

(21) Ghosh, S.; Ranjini, A. S.; Pandey, R.; Das, P. K. First Hyperpolarizability of Bacteriorhodopsin, Retinal and Related Molecules Revisited. *Chem. Phys. Lett.* **2009**, *474*, 307–310.

(22) Hendrickx, E.; Clays, K.; Persoons, A.; Dehu, C.; Bredas, J. L. The Bacteriorhodopsin Chromophore Retinal and Derivatives: An Experimental and Theoretical Investigation of the Second-Order Optical Properties. *J. Am. Chem. Soc.* **1995**, *117*, 3547–3555.

(23) Bishop, D. M.; Luis, J. M.; Kirtman, B. Additional Compact Formulas for Vibrational Dynamic Dipole Polarizabilities and Hyperpolarizabilities. *J. Chem. Phys.* **1998**, *108*, 10013–10017.

(24) Bishop, D. M.; Norman, P. In *Handbook of Advanced Electronic and Photonic Materials*; Nalwa, H. S., Ed.; Academic Press: San Diego, 2001; Vol. 9; pp 1–62.

(25) Ekström, U. XCFun Library. 2010; http://www.admol.org/xcfun.

(26) Dalton. 2011; a molecular electronic structure program, see http://www.daltonprogram.org.

(27) Bast, R.; Thorvaldsen, A. J.; Ringholm, M.; Ruud, K. Atomic Orbital-Based Cubic Response Theory for One-, Two-, and Four-Component Relativistic Self-Consistent Field Models. *Chem. Phys.* **2009**, *356*, 177–186.

(28) Becke, A. D. Density-Functional Exchange-Energy Approximation with Correct Asymptotic Behavior. *Phys. Rev. A* **1988**, *38*, 3098–3100.

(29) Lee, C. T.; Yang, W. T.; Parr, R. G. Development of the Colle-Salvetti Correlation-Energy Formula into A Functional of the Electron Density. *Phys. Rev. B* **1988**, *37*, 785–789.

(30) Stephens, P. J.; Devlin, F. J.; Chabalowski, C. F.; Frisch, M. J. Ab Initio Calculation of Vibrational Absorption and Circular Dichroism Spectra Using Density Functional Force Fields. *J. Phys. Chem.* **1994**, *98*, 11623–11627.

(31) Champagne, B.; Perpete, E. A.; van Gisbergen, S. J. A.; Baerends, E. J.; Snijders, J. G.; Soubra-Ghaoui, C.; Robins, K. A.; Kirtman, B. Assessment of Conventional Density

Functional Schemes for Computing the Polarizabilities and Hyperpolarizabilities of Conjugated Oligomers: An Ab Initio Investigation of Polyacetylene Chains. *J. Chem. Phys.* **1998**, *109*, 10489–10498.

(32) Sałek, P.; Vahtras, O.; Helgaker, T.; Ågren, H. Density-Functional Theory of Linear and Nonlinear Time-Dependent Molecular Properties. *J. Chem. Phys.* **2002**, *117*, 9630–9645.

(33) Sałek, P.; Helgaker, T.; Vahtras, O.; Ågren, H.; Jonsson, D.; Gauss, J. A Comparison of Density-Functional-Theory and Coupled-Cluster Frequency-Dependent Polarizabilities and Hyperpolarizabilities. *Mol. Phys.* **2005**, *103*, 439–450.

(34) Jacquemin, D.; Perpete, E. A.; Scalmani, G.; Frisch, M. J.; Kobayashi, R.; Adamo, C. Assessment of the Efficiency of Long-Range Corrected Functionals for Some Properties of Large Compounds. *J. Chem. Phys.* **2007**, *126*, 144105.

(35) Sekino, H.; Maeda, Y.; Kamiya, M.; Hirao, K. Polarizability and Second Hyperpolarizability Evaluation of Long Molecules by the Density Functional Theory with Long-Range Correction. *J. Chem. Phys.* **2007**, *126*, 014107.

(36) Schäfer, A.; Huber, C.; Ahlrichs, R. Fully Optimized Contracted Gaussian Basis Sets of Triple Zeta Valence Quality for Atoms Li to Kr. *J. Chem. Phys.* **1994**, *100*, 5829–5835.

(37) Sadlej, A. J. Medium-Size Polarized Basis Sets for High-Level Correlated Calculations of Molecular Electric Properties. *Coll. Czech Chem. Soc.* **1988**, *53*, 1995–2016.

(38) Champagne, B.; Perpète, E. A.; André, J.-M. Vibrational Polarizability of Polyacetylene Chains. *J. Chem. Phys.* **1994**, *101*, 10796–10807.

(39) Champagne, B.; Perpète, E. A.; van Gisbergen, S. J. A.; Baerends, E.-J.; Snijders, J. G.; Soubra-Ghaoui, C.; Robins, K. A.; Kirtman, B. Assessment of Conventional Density Functional Schemes for Computing the Polarizabilities and Hyperpolarizabilities of

Conjugated Oligomers: An Ab Initio Investigation of Polyacetylene Chains. *J. Chem. Phys.* **1998**, *109*, 10489–10498.

Graphical TOC Entry